Three-Dimensional Dynamic Self-Assembly of Spinning Magnetic Disks: Vortex Crystals

Bartosz A. Grzybowski*,† and George M. Whitesides*,‡

Harvard University, Department of Chemistry and Chemical Biology, 12 Oxford Street, Cambridge, Massachusetts 02138

Received: July 23, 2001; In Final Form: October 10, 2001

This paper describes dynamic self-assembly of millimeter-sized, magnetized disks floating at two parallel interfaces and spinning under the influence of a rotating, external magnetic field. All disks experience a central, confining magnetic potential, and interact with one another hydrodynamically both in the plane of the interface, and between the interfaces. The interactions between the disks spinning on different interfaces are repulsive for low rotational speeds, and attractive for high rotational speeds. The interplay between magnetic and hydrodynamic forces acting in the system leads to the formation of quasi three-dimensional, ordered aggregates. Changing the rotation speeds of the disks can reversibly change the morphologies of these aggregates.

Dynamic self-assembly (DySA),[1−3] that is, self-assembly in nonequilibrium systems[4,5] that organize only when dissipating energy, is fundamentally important both through its relevance to living systems, and for practical applications in adaptive[6,7] ("smart") structures or materials, i.e., structures whose mode of organization and properties depend on the energy flux through the system. Dynamic self-assembly or self-organization are often studied in systems that spontaneously develop spatial order; these systems are usually two-dimensional (2D) or quasi-2D (reaction−diffusion systems,[8,9] Benard convection,[10] and sandpiles[11]). Although the extension to three dimensions is often difficult (and is sometimes impossible), it is a necessary precondition to understanding DySA and expanding the scope of its potential applications.

We have recently described[12,13] a dynamic system of millimeter-sized, magnetized disks rotating at a liquid−air interface, in which the interplay between magnetic and hydrodynamic forces leads to the formation of regular, 2D patterns. Here, we describe an analogous system in which self-assembly involves disks spinning on two parallel interfaces and interacting with one another by three-dimensional (3D) hydrodynamic forces. Under the influence of the external, rotating magnetic field, all magnetized disks in this system spin with angular velocity ω equal to that of the external magnet. An average centrosymmetic magnetic force attracts the disks toward the axis of rotation of the magnet, and pairwise hydrodynamic forces repel them from one another. In addition, the objects spinning on different interfaces interact with each other through vortex−vortex interactions, which can be tuned from repulsive to attractive by adjusting ω (Figure 1b). The combination of the vortex−vortex interactions in-plane and between planes, and a central magnetic potential, gives raise to ordered 3D structures.

This paper is divided in two parts: (i) in the first part, we characterize the interactions acting in the system, and give their qualitative theoretical description; (ii) in the second part, we describe the aggregates that form from disks spinning on two parallel fluid interfaces, and discuss the effects that control their morphologies.

* To whom correspondence should be addressed.
† E-mail: bgrzybowski@gmwgroup.harvard.edu.
‡ E-mail: gwhitesides@gmwgroup.harvard.edu.

Aside from its relevance to the issues of dynamic self-organization, we believe that this kind of system can be useful as a model to study the hydrodynamic effects in arrays of vortices, such as those recently observed in Bose−Einstein condensates[14,15] and superconductors.[16] We also envision potential practical uses in applications in which regular arrays of objects are sought (e.g., photonics), provided that smaller particles can be shown to exhibit similar behaviors.

Experimental Setup

Figure 1a outlines the experiment. A permanent bar magnet (KIKA Labortechnik) of dimensions 5.6 cm × 4 cm × 1 cm rotated with angular velocity ω (∼200−1200 rpm) below a dish containing two immiscible liquids forming two layers: the bottom layer of perfluorodecalin (PFD), and the top layer of 3:1 by volume solution of ethylene glycol (EG) and water.[17] The magnet was magnetized along its longest dimension and had magnetization $M \sim 1000$ G/cm^3. The distance between the upper face of the magnet and the interface between the PFD and the EG/H_2O mixture was $H \sim 30$ mm, and the thickness of the EG/H_2O layer was $h \sim 1-6$ mm.

The circular disks were fabricated by a two-step procedure. First, hollow polyethylene tubing (∼1 mm i.d., ∼2 mm o.d., Intramedic) was filled with a mixture of poly(dimethylsiloxane) (PDMS, Dow Corning) containing magnetite (15 wt %), and the polymer was allowed to cure at 60 °C for 2 h. The resulting composite was cut into slices ∼400 μm thick using a custom-made precision cutter.[18] Disks were placed on the interface between air and EG/H_2O, and on that between EG/H_2O and PFD, and were immersed in the EG/H_2O layer.

The images of the aggregates were taken with a CCD camera interfaced to a VHS recorder; these images were subsequently digitized using ScionImage software. The flowlines in the EG layer were visualized by adding droplets of a solution of crystal violet in a 3:1 mixture of ethylene glycol and water.

Theory

(i) Forces Acting Within One Layer. Under the influence of the magnetic field produced by the rotating magnet, all of the disks floating on the two interfaces experience a centrosymmetric force F_m directed toward the axis of rotation of the

10.1021/jp012819k CCC: $22.00
Published on Web 01/19/2002

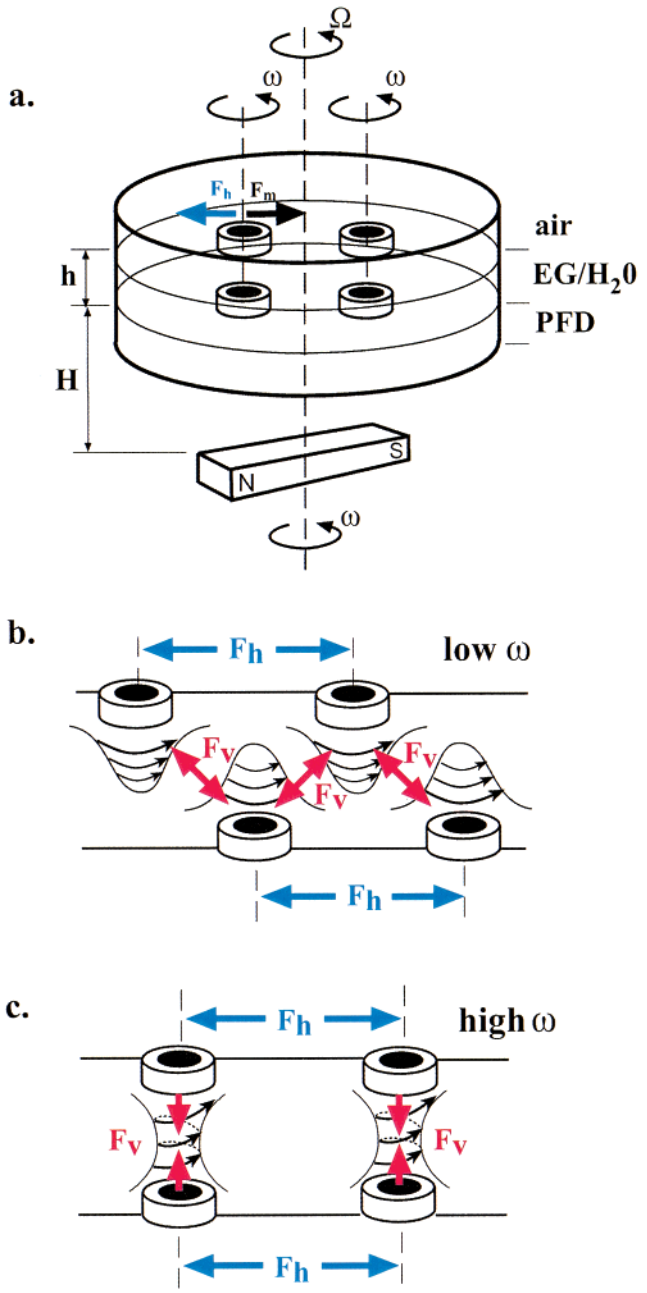

Figure 1. (a) Shown is the scheme of the experimental arrangement. All disks are attracted toward the axis of rotation of the magnet by a centrosymmetric magnetic force F_m. Within the plane of each interface, disks repel one another by pairwise hydrodynamic forces F_h (blue arrow). (b,c) Disks spinning on different interfaces interact hydrodynamically. At low rotational speeds (b), the "vertical" interactions F_v (indicated by red arrows) are repulsive. Patterns of disks that form on both interfaces minimize these repulsions by orienting "staggered" with respect to each other. (c) At high rotational speeds, the interactions between disks spinning on different interfaces are attractive. Disks form pairs connected by columnar vortices; the patterns formed on the upper and on the lower interfaces are "eclipsed."

magnet. With the magnet used in our experiments, and for distances between the top face of the magnet and an interface $H \sim 3-4$ cm, this magnetic force is a slowly varying, approximately linear, function of position within an interface:[13] $F_m = -c_m|r|\hat{r}$, where c_m is a constant. Also, if the distance h between the interfaces is small relative to H, the value of this force is approximately equal on both interfaces.

Because the magnetic moments of the disks interact with the magnetic moment of the external rotating magnet, the disks spin around their axes at an angular velocity ω equal to that of the magnet. The fluid motion associated with spinning results in repulsive hydrodynamic interactions F_h between the disks. We have previously suggested[12,13] that the origin of these repulsions can be explained using ideas from low (but not zero)-Reynolds-number hydrodynamics. According to this analysis, the hydrodynamic repulsion F_h^{ij} exerted by a disk of radius a_j on a disk of radius a_i depends on the radii of the disks, the distance d_{ij} between their centers, the rotational speed ω, and the density of the fluid ρ: $F_h^{ij} \propto \rho\omega^2 a_j^3 a_i^4/d_{ij}^3$. The force on disk i acts along the direction of d_{ij} and away from disk j. The interplay between attractive and repulsive interactions between the disks floating on the same interface leads to formation of patterns.

The magnitudes of magnetic dipole−dipole forces F_m^{ij} acting between the disks are small compared to the centrosymmetric magnetic force F_m and to the pairwise hydrodynamic interactions F_h^{ij}. In the presence of the external magnetic field, each disk acquires a magnetic dipole of magnitude $m = \mu_o V\chi H$, where μ_0 is the magnetic permeability of vacuum, V is the volume of a disk ($\sim$1.3 mm^3), χ is its effective magnetic susceptibility, and H is the strength of the magnetic field in the plane of the interface ($\mu_0 H \sim 0.05$ T). Since the magnetite particles are uniformly distributed in the PDMS matrix and no long-range order exists between magnetic domains (so that disks are superparamagnetic rather than ferromagnetic), the value of χ can be estimated from a low-field expansion of the Langevin function:[19] $\chi(2\chi + 3)/(\chi + 1) = \pi\phi\mu_0 M_S^2 l^3/6kT$. In this equation, ϕ is the volume fraction of magnetite in the disks ($\sim$0.01), M_S is the saturation magnetic moment of magnetite ($\sim 0.4 \times 10^6$ A/m) and l is the typical size of a magnetite grain ($\sim$100 Å). The value of χ is estimated at $\sim$0.1, and the induced magnetic moment is $m \sim 6.5 \times 10^{-12}$ T m^3. The magnitude of the force F_m^{ij} acting between the disks is calculated by taking the gradient of the interdisk potential:

$$|F_m^{ij} = |\partial U(r,\theta)/\partial r| = |\frac{3m^2}{4\pi\mu_0}\frac{1-3\cos^2\theta}{r^4}|$$

where r is the distance between the centers of the disks, and θ is the angle between the line joining these centers and the direction of the external field. Even if magnetic moments of all disks were aligned at all times, the magnitude of F_m^{ij} would not exceed $\sim$0.002 dynes. On the other hand, the centrosymmetric magnetic force F_m calculated from the product of the induced magnetic moment and the gradient of the magnetic field at the location of the disk (conservatively estimated at $\sim$1 G/cm) is $\sim$0.065 dynes: more than 30 times larger than F_m^{ij}. Also, we have previously shown[20] that, at short separations $r < \sim 5$ mm, the hydrodynamic forces F_h^{ij} are on the order of tenth of dynes to dynes; the magnetic dipole−dipole forces are thus negligible for all values of r, and are not included in the analysis of self-assembly in our system. We briefly mention, however, that the relative magnitude of these forces increases with decreasing size of and separation between spinning particles, and they do influence self-assembly on the micrometer scale. In experiments with heavily ($\sim$35 wt %) magnetically doped 50 μm disks, we observed formation of "chain" aggregates indicative of large magnetic dipole−dipole forces between the spinning particles.

(ii) Experimental Characterization of Forces Acting Between the Layers. Spinning disks create so-called Taylor vortices[21] in the fluid above and below the plane of the interface on which they float. These vortex motions give rise to hydrodynamic, "vertical" forces F^v between disks spinning on different interfaces. To characterize these interactions, we

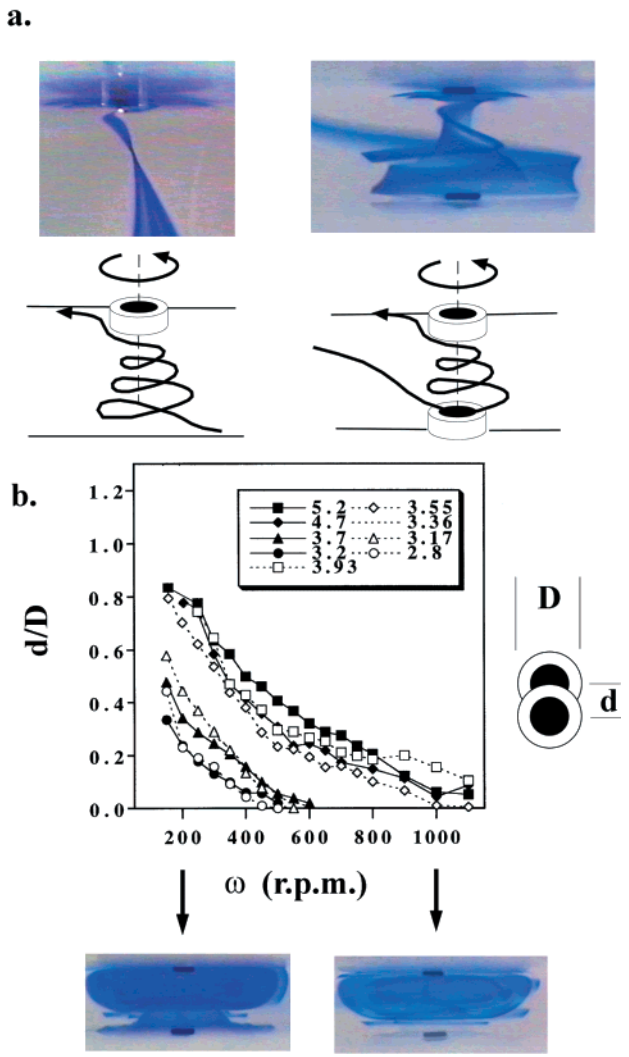

Figure 2. (a) Shown are the flowlines in the EG layer under one disks spinning on the EG/air interface (left), and between two disks (right) spinning on EG/air and EG/PFD interfaces, respectively. The disks used in these experiments were 1.57 mm in diameter and rotated at 600 rpm. The flowlines were visualized using a mixture of EG and water of the composition identical with that of the EG layer and colored with crystal violet. The schematic pictures illustrate the streamlines produced by both rotating disks. The graph in (b) gives the dependence of the relative displacement *d/D* of the disk centers as a function of the rotational speed of the magnet. The solid markers correspond to disks of diameter $D = 2.08$ mm, and the open markers to disks of $D = 1.57$ mm. The thicknesses of the EG layer are given in millimeters in the legend. The insert pictures illustrate how the rate of transfer of the liquid (pumping) from the lower to the upper interface varies with ω. At low rotational speeds, the colored liquid resides near the lower interfaces for several minutes, while at high rotational speeds it is pumped onto the upper interface within several seconds.

performed a set of experiments in which we (i) visualized the flowlines in the EG layer, and (ii) monitored the relative position of interacting disks for various values of controlling parameters (ω, *D*, *h*).

The Taylor vortex produced by a single disk spinning on the interface between air and EG/H_2O is illustrated in the left picture in Figure 2a. The streamlines trace a spiral directed toward the interface so that the disk acts as a pump transferring the liquid from the bulk below it onto the interface. We observed that the rate of this, so-called, Ekman pumping[21] increases with increasing rotational speed of the disk. For a disk spinning at the interface between PFD and EG/H_2O, the streamlines point toward the PFD layer, and the liquid is pumped from the bulk onto the interface. When two spinning disks on different interfaces interact (Figure 2a, right), a columnar vortex forms between the lower and the upper disks. The layers are "connected" by a rotating column with the liquid first being drawn onto the lower disk, and then pumped upward onto the upper disk and, eventually, onto the upper interface. We point out that although each separated disk pumps liquid toward the interface on which it is rotating, pumping between connected disks is *directional*, i.e., from the lower to the upper interface. This asymmetry reflects the differences in surface tensions of the liquid−liquid and the liquid−air interfaces (and, unfortunately, makes the exact analytical description of our system formidably difficult).

We quantified the strength of the vertical interaction between two rotating disks on different interfaces. To describe the mutual orientation of these disks, we defined a quantity *d/D* ("relative displacement"), in which *d* is the horizontal component of the distance between the centers of the disks, and *D* is the disk diameter. If the distance between the interfaces is large ($h >$ 20 mm), the interaction between the disks is negligible, and they experience only the magnetic attraction that draws them toward the axis of rotation of the magnet. Because both noninteracting disks have their axes of rotation coinciding with the axis of rotation of the magnet, their relative displacement *d/D* is equal to zero.

When the thickness of the EG layer is decreased, the disks begin to interact. Figure 2b shows the dependence of *d/D* on the rotational speed ω for different values of *h* and *D*. At low rotational speeds ($\omega \sim 200$ rpm), *d/D* is large (disks are pushed away from each other), and decreases monotonically with increasing ω (disks are drawn onto each other). In other words, the vertical interaction between the disks is repulsive at low rotational speeds, and attractive at high values of ω.

When the rotational speed of the interacting disks is increased, the rate of liquid transfer from the lower to the upper interface increases. The photographs in Figure 2b were taken ~1 min after a drop of colored EG/H_2O mixture was introduced onto the interface between PFD and EG/H_2O, approximately 1 cm from the rotating disk. When the disks rotate slowly (left picture), the colored liquid is pumped onto the upper layer slowly, and resides near the lower interface for several minutes. When the disks rotate rapidly (right picture), the pumping is much faster, and the dye is cleared from the bottom interface within few seconds.

The displacement *d/D* also depends on the disk diameter *D* and the thickness *h* of the EG/H_2O layer. We hypothesized that if both *D* and *h* were scaled by the same factor, the nature of the vertical interaction should not change; therefore, the value of *d/D* at a given ω (and for a given solvent) should depend only on the ratio *h/D*. To test this hypothesis, we plotted the displacement *d/D* as the function of *h/D* for several values of *h* and two values of *D* (1.57 mm and 2.08 mm). The curves in Figure 2b correspond to different thicknesses *h* of the EG layer (given in millimeters in the legend). Solid markers correspond to disks of diameter $D = 2.08$ mm, and the open markers to disks of $D = 1.57$ mm. For a given ratio *h/D* (e.g., solid triangles and open triangles), *d/D* is roughly constant.

The curves in the graph form two distinct families: the lower ones (circles and triangles) have $h/D \sim 2$, whereas the upper ones (squares and rhomboids) have $h/D \sim 3$. The ratio of values of *d/D* for these two families is roughly equal to 3, and the dependence of *d/D* on *h/D* is thus stronger than linear. Therefore, the disks are considerably easier to align if they spin on closely spaced interfaces; if the distance between the interfaces is large, higher rotation speeds are needed to achieve alignment.

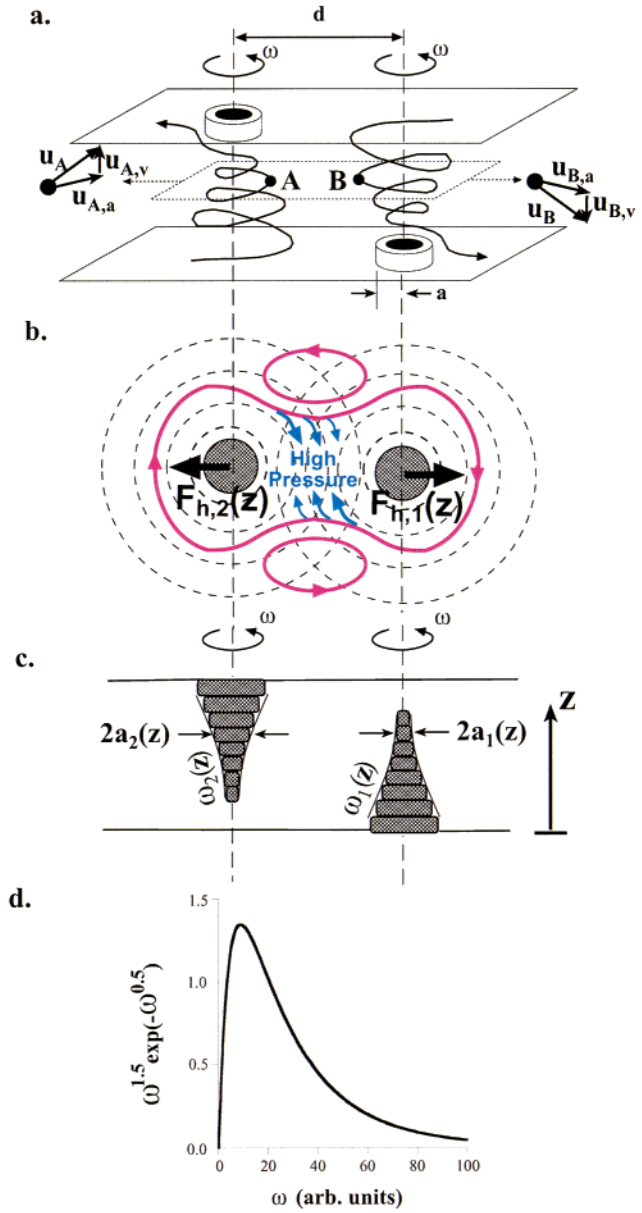

Figure 3. (a−c) Illustration of the origin of repulsive component of the interaction between separated vortices produced by disks spinning on different interfaces (see Text for details). The graph in (d) shows qualitatively the dependence of the magnitude of this repulsion on the rotational speed of the disks.

In summary, the vertical interaction between spinning disks: (i) has attractive and repulsive components, (ii) the repulsive component dominates at low rotational speeds, (iii) the attraction between spinning disks increases with ω, (iv) stronger attraction correlates with increased rate of liquid transfer (pumping) from the lower toward the upper interface, (v) the strength of the interaction depends on the ratio h/D.

(iii) Qualitative Description of the Vertical Interaction. The fluid mechanics of a system of two rotating parallel plates have been studied for many decades.[22,23] Unfortunately, even for the simplest arrangement—two finite circular plates with a common axis of rotation—there are no known analytical solutions. In our system, where the axes of rotation of the disks do not coincide and can vary with ω, a quantitative fluid-mechanical description presents formidable difficulties. We, therefore, restrict ourselves to a simple *qualitative* argument to rationalize the interaction between the spinning disks.

Consider two identical disks of radii a spinning with angular velocity ω on parallel interfaces with their axes of rotation

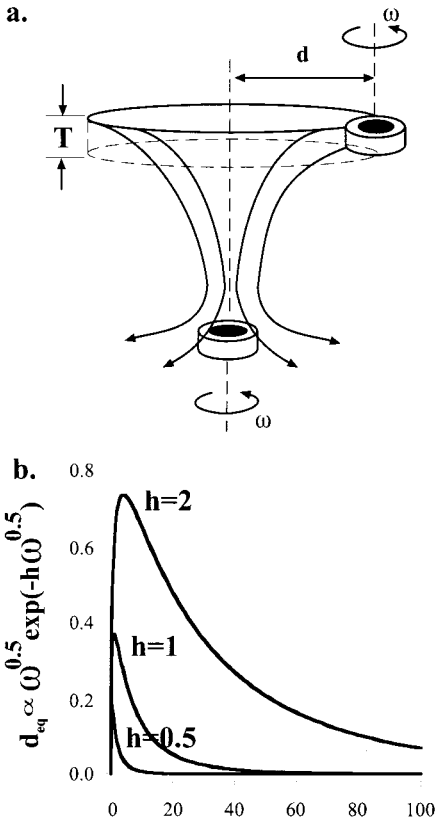

Figure 4. (a) Illustration of the origin of the attractive component of vertical vortex−vortex interaction (see Text for details). The graph in (b) shows a qualitative profile of the equilibrium separation d_{eq} between the centers of two disks as a function of their rotational speed.

separated by a distance d larger than the disk diameter ("separated disks", Figure 3a). Each disk has a Taylor vortex associated with it. The flowlines within each vortex trace helical paths. In the following, we argue that the azimuthal components of velocity (i.e., parallel to the plane of the interface, and tangential to the flowlines) in each Taylor vortex give rise to repulsive interactions between the disks, while the vertical motions of the fluid account for the attraction between the disks (Figure 3).

Repulsive Interaction. We choose two points A and B lying on the same horizontal plane, and located on two flowlines associated with different disks. The horizontal azimuthal ($u_{A,a}$ and $u_{B,a}$) and vertical ($u_{A,v}$ and $u_{B,v}$) components of the velocities of fluid elements at these loci are schematically drawn in Figure 3a. The azimuthal components have the same sense of rotation; the circular flowlines within the horizontal plane containing A and B are qualitatively similar to those produced by two separated disks spinning at this plane. Using this analogy, we will treat the horizontal hydrodynamic interactions between the fluid elements in the AB plane, as if they were produced by two fictitious disks spinning at this plane and coaxial with the real disks spinning on the interfaces (Figure 3b).

We first find the dependence of the radii of such "disks" on the distance z from the lower interface (Figure 3c). It has been shown[24] that for an infinite disk rotating with angular velocity ω, the angular velocity of the liquid above it decays approximately as $\omega(z) \propto \exp(-\text{constant} z\omega^{1/2})$, where z is the elevation above the plane of the disk; numerical simulations[25] suggest that a qualitatively similar relationship holds when the size of a disk and the thickness of a liquid layer are finite. Using this approximation, the flow-field at elevation z created by the disk spinning at $z = 0$ (lower interface) can be regarded as that

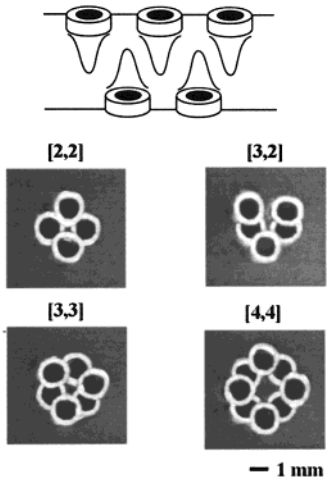

Figure 5. Shown are dynamic patterns formed by small numbers (less than 5) of 1.57 mm disks spinning on two parallel interfaces ($h = 2.5$ mm) at $\omega = 500$ rpm. Within each interface, the disks form patterns observed in one-layer systems with the same numbers of disks. The patterns that form on different interfaces are oriented "staggered" with respect to each other; the schematic diagram shows that this orientation minimizes repulsions between the disks.

created by an imaginary disk of radius[26] $a_1(z) \propto a \exp(-\text{constant}z\omega^{1/2})$ spinning at z with angular velocity ω. By similar argument, the flow field in the z plane created by the disk spinning at $z = h$ (upper interface) can be approximated by that created by an imaginary disk of radius $a_2(z) \propto a \exp(-\text{constant}_2(h - z)\omega^{1/2})$ rotating at angular velocity ω. The magnitude of the repulsive hydrodynamic force exerted by disk 1 on disk 2 is given by $F_{h,1}(z) \propto \rho\omega^2 a_1^3(z)a_2^4(z)/d^3$, and the total repulsive force F_R between the Taylor vortices is obtained by summing repulsive forces between imaginary disks at all elevations within the liquid layer:

$$F_R(d) \propto \int_{z=0}^{z=h} \rho\omega^2 a_1^3(z)a_2^4(z)/d^3 \, dz \qquad (1)$$

Integrating and neglecting small exponential terms, F_R can be rewritten as

$$F_R(d) \propto \omega^{3/2} \exp(-4\text{constant}_2 h\omega^{1/2})/d^3 \qquad (2)$$

The qualitative dependence of this force on the rotational speed is shown in Figure 3d: for small values of ω, the repulsion grows with angular speed until it reaches a maximum, and it decays (approximately exponentially) for high values of rotational speeds.

Attractive Interaction. As ω becomes larger, the repulsion described by eq 2 becomes smaller; at the same time, an *attraction* between disks becomes more important. Consider the flux toward the disk spinning on the lower interface (Figure 4a). The quantity of fluid Q flowing toward this disk depends on the rotational speed ω and the radius a of the disk:[24] $Q \propto a^2\omega^{1/2}$. As confirmed by direct observation, the fluid is pumped onto the lower disk from the region near the upper interface. To simplify the argument, we assume that this region is a layer of constant thickness T, and consider the flow within this layer that is directed toward the axis of rotation of the lower disk (the angular component of the flow does not contribute to the transport of liquid onto lower disk). By continuity, the quantity of liquid entering a cylindrical slab of radius d and thickness T near the upper interface per unit time must be equal to Q: $2\pi Td\dot{d} = Q$. Therefore, the radial (directed toward the axis of rotation of the lower disk) velocity of the liquid near the interface is $\dot{d} = Q/2\pi Td$. The radial component of pressure in the liquid is found using the Bernoulli's equation:[27] $p(d) \propto (Q/d)^2$. This pressure gradient gives rise to a force F_A that acts on a neutraly buoyant disk floating on the upper interface and attracts it toward the axis of rotation of the lower disk: $F_A(d) \propto (Q/d)^2 \propto \omega/d^2$ (a similar force acts on the lower disks as the result of the liquid transfer from the lower interface toward the upper spinning disk). This attractive force increases monotonically with increasing rotational speed of the disks.

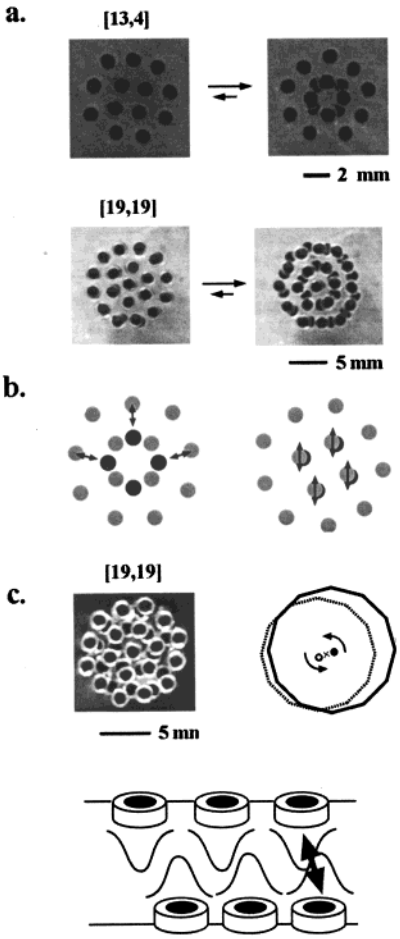

Figure 6. (a) Staggered conformations in large aggregates are metastable; the assemblies on different interfaces periodically "slide" past each other. (b) The arrows in the schematic diagram indicate unfavorable hydrodynamic repulsions in both "staggered" and "eclipsed" conformations of [13,4] aggregate. (c) When the EG layer is made thicker (2.5 mm in a vs 5 mm in c), the magnitude of vertical hydrodynamic repulsions decreases. Because of stronger magnetic confinement on the lower layer (the layer closer to the magnet), the lower aggregate is more compact than the upper one by ~10%. Weakly interacting aggregates of different shapes do not equilibrate, and continually move with respect to each other precessing around the axis of rotation of the magnetic field (diagram on the right). Because the interdisk spacings are mismatched, aggregates cannot "lock" as in (a). The rotational speed of the disks was 500 rpm in all experiments.

Balance of Forces. The equilibrium separation between the axes of rotation of the disks is defined by the balance of the attractive force F_A and the repulsive force F_R:

$$\omega/d_{eq}^2 = \text{constant}_3\omega^{3/2} \exp(-4\text{constant}_2 h\omega^{1/2})/d_{eq}^3 \qquad (3)$$

$$d_{eq} \propto \omega^{1/2} \exp(-4\text{constant}_2 h\omega^{1/2}) \qquad (4)$$

The qualitative dependence of the equilibrium separation on the rotational speed is illustrated in Figure 4b. At low values of ω,

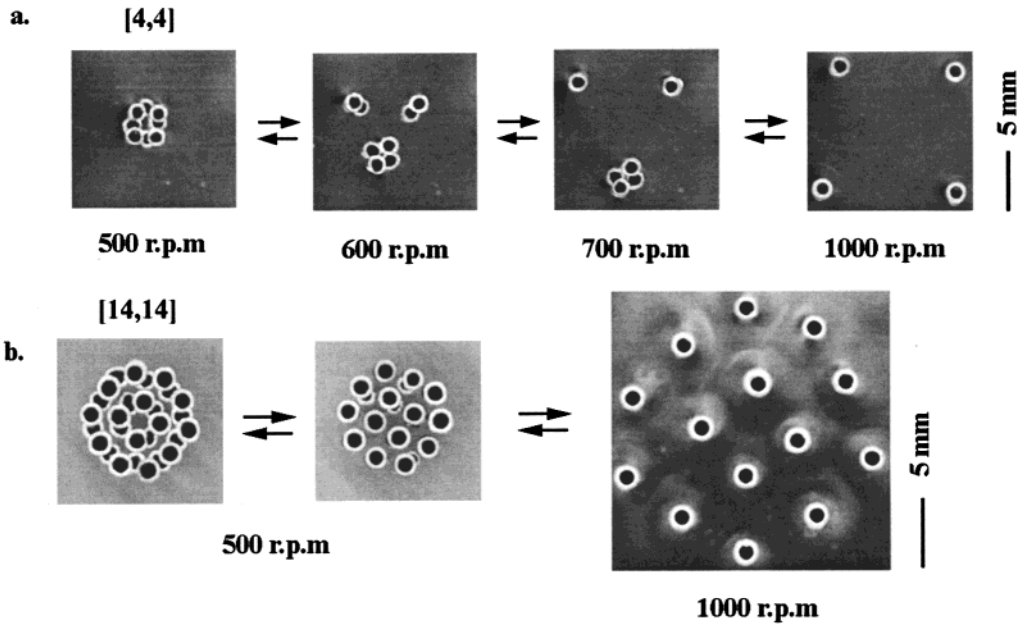

Figure 7. Illustration of the effect of the angular velocity ω on the morphology of the dynamic patterns. At low ω ($\sim$300−500 rpm), the patterns are either stable "staggered" structures (a), or interconvert between "staggered" and "eclipsed" conformations (b). As the rotational speed increases, the interactions between the disks on different interfaces become attractive: the original patterns disappear, and pairs of disks (one from each interface) form. At $\omega \sim 1000$ rpm, all disks are oriented in pairs connected by columnar vortices. The hydrodynamic repulsive force generated by such a pair is much stronger than that generated by a single disk. As the result, the stable pattern that forms has the symmetry of the original pattern, but its size is more than twice of that expected for a single-layer aggregate at $\omega = 1000$ rpm.

the separation between the disks increases with ω until it reaches a maximum; past this maximum d_{eq} decreases approximately exponentially with ω. Also, for a given value of rotational speed, the model predicts an exponential decrease in d_{eq} with increasing h. We experimentally observed a stronger-than-linear decrease in the equilibrium separation of disks with both h and ω (for $\omega > \sim$150 rpm). Although the values of d_{eq} at very low rotational speeds ($\omega < \sim$150 rpm) were ill-defined (due to tumbling of the disks and their tendency to follow the poles of a slowly rotating magnet), we observed an increase in d_{eq} with increasing ω in experiments performed in pure EG and with disks of higher magnetic content (in which tumbling and precession were eliminated).

Self-Assembling Systems

(i) Two-Layered Aggregates at Low Rotational Speeds. Figure 5 shows the dynamic patterns formed by different numbers of 1.57 mm disks spinning on two interfaces. The notation [x,y] gives the number x of disks on the upper interface, and the number y of disks on the lower interface. In all experiments, the disks were spinning at angular velocity $\omega =$ 400 rpm. In the plane of each interface, the disks formed patterns we have described previously[12] for the same numbers of disks rotating on a single interface. The mutual orientation of patterns on different layers depended on the size of aggregates and the distance h between the interfaces ($h = 2.5$ mm in a and b, and $h = 5$ mm in d). Small aggregates composed of up to 4 disks on each interface (Figure 5) were all stable in time. Because at low rotational speeds the vortices repel each other, the upper and lower polygons were oriented in a "staggered" fashion with respect to each other: this orientation minimized repulsions between the disks.

When the aggregates were made larger, polygons on different layers preferred staggered orientations, but they were occasionally moving (sliding) with respect to each other. The pictures in Figure 6a show two extreme orientations that interconvert in time: a transient, "eclipsed" conformation on the left, and a metastable, "staggered" conformation on the right. We suggest that the instabilities in these assemblies are caused by interactions between disks in different shells in lower and upper polygons. For instance, in the [13,4] aggregate, the hydrodynamic repulsions between the disks on the lower interface, and the four central disks of the structure on the upper interface are minimized in "staggered" orientation; this orientation, however, *maximizes* repulsions between the lower interface disks, and those in the outer shell of the upper-interface aggregate (Figure 6b, left). Conversely, the favorable, staggered orientation of the lower interface disks with respect to the outer shell of the 13-membered aggregate leads to unfavorable, "eclipsed" conformation of the central squares on both interfaces (Figure 6b, right). As the result, the system is frustrated, and cannot achieve a stable, equilibrium structure; instead, it switches between degenerate metastable states every few seconds.

When the thickness of the EG layer is increased, the repulsions between vortices on different interfaces become weaker. An aggregate on the lower interface also experiences a higher confining magnetic field than that on the upper interface; consequently, if both aggregates are composed of the same numbers of disks, the lower assembly is more compact than the upper one (Figure 6c). Weak repulsions and different interdisk spacing in both aggregates (and thus no strongly favored, symmetric conformations that would minimize pairwise repulsions between the disks) result in continuous sliding of the aggregates with respect to each other.

(ii) Two-Layered Aggregates at High Rotational Speeds: Columnar Structures. Because hydrodynamic repulsions between disks in the same interface increase with increasing ω, the aggregates on both layers become larger and less stable at high rotational speeds. The *decrease* in stability within one layer is accompanied by the *increase* in the attractive component of the vertical vortex−vortex interaction between disks in different

interfaces. Combination of these two effects modifies the morphologies of patterns.

Figure 7a illustrates the changes in the morphology of a [4,4] aggregate composed of 1.57 mm disks. Initially, at $\omega < \sim 500$ rpm, disks on each interface are arranged into ~4 mm × 4 mm squares that are staggered with respect to each other. When ω is increased to 600 rpm, this structure disintegrates, and smaller "substructures" are formed (in the picture shown in 6a - -two pairs of disks and a cluster of two pairs; note that the three substructures are arranged into a larger triangular "superstructure"). As the angular velocity of disks is increased further, the substructures composed of more than two disks dissociate. Finally, at $\omega \sim 1000$ rpm all disks are arranged in pairs and their axes of rotation are almost aligned. The liquid between two disks constituting a pair forms a columnar vortex that "glues" the disks together. The [4,4] aggregate at 1000 rpm is a square with four aligned pairs positioned in its vertexes ("eclipsed" structure). Because the aligned disks impart high angular velocity to the liquid between them, the hydrodynamic repulsion between coupled pairs of disks spinning on two interfaces is much stronger than between single disks: as the result, the "eclipsed" aggregate is much larger (by a factor of ~2.5) than the original "staggered" structure.

The transition to expanded, columnar structures is observed also in larger systems. Figure 5b shows the low- and high-ω structures of [14,14] aggregates. The structure forming at 1000 rpm preserves the symmetry of a 14-membered aggregate formed by disks on one interface at low rotational speeds, but its size is approximately 2.5 times larger. We briefly (and somewhat provocatively) note that the alignment of disks within pairs accompanied by the expansion of the "superstructure" can be loosely described as a (second-order) phase transition. The change in ordering is reminiscent of that occurring during crystallization; the expansion of the structure accompanying the change prompts a pictorial analogy to the freezing of water.

Conclusions and Outlook

The vertical interactions between vortices created by disks spinning on parallel interfaces are the basis of a system of particles that form a remarkable series of structures by quasi three-dimensional dynamic self-assembly. The new and particularly interesting feature of these interactions is that they have (in contradistinction to purely repulsive interactions within the same interface) both repulsive and attractive components, each dominant over a different range of controlling parameter ω. This property allows modifications of the morphologies of the self-assembled aggregates. In principle, the horizontal and vertical interactions can be tuned selectively: the former by adjusting the cross-section of the spinning object, and the latter by modifying its shape in the direction perpendicular to the plane of the interface; such selectivity would lead to morphologies other than the "eclipsed" and "staggered" ones described here. Although the layered aggregates we prepared bear visual analogies to crystalline lattices, they are, admittedly, not fully three-dimensional structures. We are currently working on multilayered (up to 5 interfaces) liquid systems by matching densities and miscibilities of the liquids.

We believe this system can be used in two areas: (i) In hydrodynamics, the spinning disks (or objects of other shapes) can help study the 3D interactions between co-rotating vortices or vortex patches.[28,29] The theoretical description and controlled experimental realization of vortex−vortex interactions in three dimensions are often prohibitively complicated: the experimental simplicity of our system might offer a remedy to these problems. (ii) In self-assembly and materials science, the systems of spinning objects can serve as precursors for open lattices to be used in photonic band gap materials or molecular sieves. The potential of our system in this application would, however, only be realized, if the sizes of the objects were made two or 3 orders of magnitude smaller than they presently are; we are currently working on systems of spinners of sizes ~100 μm.

Acknowledgment. This work has been supported by the U.S. Department of Energy (Award 00ER45852).

References and Notes

(1) Mikhailov, A. S.; Ertl, G. *Science* **1996**, *272*, 1596.

(2) Cross, M. C.; Hohenberg, P. C. *Rev. Mod. Phys.* **1993**, *65*, 851.

(3) Jakubith, S.; Rotermund, H. H.; Engel, W.; Von Oertzen, A.; Ertl, G. *Phys. Rev. Lett.* **1990**, *65*, 3013.

(4) Glansdorff, P.; Prigogine, I. *Thermodynamic Theory of Structure, Stability and Fluctuations*; Wiley: New York, 1971.

(5) Nicolis, G.; Prigogine, I. *Self-Organization in Nonequilibrium Systems*; Wiley: New York, 1977.

(6) Kannari, F.; Takei, N.; Shiozawa, M. *Rev. Laser Eng.* **2000**, *28*, 479.

(7) Alstrom, P.; Stassinopoulos, D. *Phys. Rev. E* **1995**, *51*, 5027.

(8) Epstein, I. R.; Showalter, K. *J. Phys. Chem.* **1996**, *100*, 13132.

(9) Nijhout, H. F., Nadel, L., Stein. D., Eds., *Pattern formation in the Physical and Biological Sciences*; Addison-Wesley: New York, 1997.

(10) Koschmeider, E. L. *Bénard Cells and Taylor Vortices*; Cambridge University Press: Cambridge, 1993; pp 1−194.

(11) Jaeger, H. M.; Nagel, S. R. *Science* **1992**, *255*, 1523.

(12) Grzybowski, B. A.; Stone, H. A.; Whitesides, G. M. *Nature* **2000**, *405*, 1033.

(13) Grzybowski, B. A.; Xingyu, J.; Stone, H. A.; Whitesides, G. M. *Phys. Rev. E* **2001**, *46*, 11603.

(14) Feder, D. L.; Clark, C. W.; Schneider, B. I. *Phys. Rev. A* **2000**, *60*, 1601.

(15) Fedichev, P. O.; Shlyapnikov, G. V. *Phys. Rev. A* **1999**, *60*, 1779.

(16) Palacios, J. J. *Phys. B* **1998**, *258*, 610.

(17) Kinematic viscosity of the mixture affected the stability of the aggregates. In liquids of low viscosities ($\nu < \sim 3$ cp), the flows created by spinning disks were often turbulent, and the self-assembled aggregates were unstable. If the viscosity was too high ($\nu > \sim 50$ cp), the magnetic torque was to small to spin the disks. Most stable structures were observed in liquids of intermediate kinematic viscosities, such as the 1:1 mixture of EG and water.

(18) The cutter was build from three translational stages. Two of the stages were stacked on top of each other and served as an *xy* platform, on which the tubing was placed. The third stage was free to move in the direction perpendicular to the plane of the platform, and had a fine razor blade glued to it; this blade was used to cut the tubing.

(19) Rosensweig, R. E. *Ferrohydrodynamics*; Dover: New York, 1997; Chapter 2.

(20) Grzybowski, B. A.; Stone, H. A.; Whitesides, G. M. *Proc. Nat. Acad. Sci.* **2001**. Submitted for publication.

(21) Tritton, D. J. *Physical Fluid Mechanics*; Clarendon Press: Oxford, 1988; Chapter 16.

(22) Batchelor, G. K. *Q. J. Mech. Appl. Math.* **1951**, *4*, 29.

(23) Dijkstra, D.; Van Heijst, G. J. F. *J. Fluid Mech.* **1983**, *128*, 123.

(24) Schlichting, H. *Boundary Layer Theory*; McGraw-Hill: New York, 1979; pp 102−107.

(25) Brady, J. F.; Durlofsky L. *J. Fluid Mech.* **1987**, *175*, 363.

(26) The angular velocity of a fluid around a 2D disk of radius a drops off quadratically with the distance from the disk r: $\omega(r) = a^2\omega(a)/r^2$. Therefore, for the same values of r and at different elevations z, $\omega(r, z)/\omega(r, 0) = a^2(z)/a^2(0)$, and $a(z) \propto a(0)\sqrt{\exp(-\text{constant}z\omega^{1/2})}$. This equation can be rewritten as $a(z) \propto a(0)\cdot\exp(-\text{constant}_2 z\omega^{1/2})$, where $const_2 = const/2$.

(27) We estimated the Reynolds number describing the motions of the fluid near the upper interface (and the disk floating on it) using the typical values of velocity $\dot{d} \sim 5$ mm/s, characteristic length scale (disks diameter) ~2 mm, and kinematic viscosity ~5−10 cm^2/s to be ~10−20. Although at this value of Re viscous effects are still present, they can be, to a good approximation, neglected permitting the use of Bernoulli equation.

(28) Havelock, T. H. *Philos. Mag.* **1931**, *11*, 617.

(29) Dritschel, D. G. *J. Fluid Mech.* **1985,** *157*, 95.